Size Effect of α,ω-Diphenylpolyenes on the Formation of Nanotubes with γ-Cyclodextrin

G. Pistolis and Angelos Malliaris*

National Centre for Scientific Research "Demokritos", Athens 15310, Greece

Received: July 11, 1997; In Final Form: November 17, 1997

We have studied the size effect of the homologues of the α,ω-diphenylpolyenes series, with two, three and four double bonds, on the formation of nanotubes with γ-cyclodextrin. The data show that only the two longest polyenes facilitate the formation of tubular structures when mixed with the γ-cyclodextrin in the appropriate solvent, while the average length of these nanotubes increases with increasing size of the diphenylpolyenes. Using computer simulations, we have examined the processes by which nanotubes form, and from computer fits we have determined the various binding constants, some with extremely large values, involved in the formation of these supramolecular structures.

I. Introduction

Cyclodextrins, and in particular the so-called α, β, and γ homologues, have attracted considerable attention during the past decade.[1] In a recent publication[2] we discussed the formation of long, rodlike structures between α,ω-diphenylhexatriene (DPH) and γ-cyclodextrin (γCD) (see structures in Scheme 1). These so-called nanotubes[3] contain up to ca. 30 cyclodextrin units interconnected by means of DPH molecules. In these structures the γCD units are understood[2,3] to be lined up along their cylindrical axis so that H-bonding interactions between the rim OH groups of neighboring γCDs are favored. The DPH molecules, on the other hand, penetrate the cavities of two neighboring γCDs, thus stabilizing, by van der Waals interactions the superstructure. The crucial contribution of both γCD−γCD and DPH−γCD interactions to the formation of nanotubes is demonstrated not only by the fact that these tubes do not form in the absence of DPH but also by the observation that when the rim hydroxyls of γCD are replaced by the non-H-bonded OCH_3 groups, or when the pH of the solvent is high enough to render H-bonding ineffective, nanotubes do not form any more.[2] The rodlike structure of these DPH-γCD aggregates has been established by several other physicochemical methods,[2,3] including light scattering and scanning tunneling microscopy.[3] Note that other rodlike structures involving cyclodextrins include catenanes,[4] rotaxanes,[4,5] polyrotaxanes,[4,6−9] nanotubular stuctures,[3,6] threaded cyclodextrins,[6] etc.

The objective of the present work was to study the effect of the length of the α,ω-diphenylpolyenes, with the general formula Ph−(CH═CH−)$_n$−Ph, on nanotube formation. For this purpose we have examined the complexation of three such molecules, viz., $n = 2-4$, with γCD in a 60/40 v/v water/glycol solvent. Note that in this type of study diphenylpolyenes play a double role; one is that of a "shaft" that enhances the binding of two neighboring γCD units, and the other is that of a fluorescent probe, which probes nanotube formation by the magnitude of its fluorescence anisotropy.[2,3] Another main point of focus of this work was to extract numerical values for the equilibrium constants involved in the formation of these elongated superstructures, since so far the few publications on this subject[2,3] deal exclusively with the qualitative aspects of nanotube formation. To this end, we have made extensive use of computer fits and simulations to obtained values for the relevant kinetic parameters.

II. Experimental Section

γ-Cyclodextrin (γCD) was purchased from Cyclolab. The Ph−(CH═CH−)$_n$−Ph diphenylpolyenes with $n = 2$ (DPB) and $n = 4$ (DPO) were obtained from Aldrich and the one with $n = 3$ (DPH) from Fluka. All chemicals were of the highest purity available, and therefore, they were used without further purification. Absorption spectra were recorded on a Perkin-Elmer Lambda-16 spectrophotometer, whereas for fluorescence, excitation, and fluorescence anisotropy measurements, we used the LS-50B Perkin-Elmer fluorometer. Fluorescence lifetimes (τ) were determined using the time-correlated single-photon counter FL900 of Edinburgh Instruments, which is capable of measuring lifetimes to 0.08 ns. The determinations of fluorescence quantum yields (Φ), and anisotropies (r), have been described elsewhere.[10] It should be mentioned here that the excitation wavelengths for the measurements of the fluorescence quantum yields were chosen to be at isosbestic points, i.e., points at which the absorption coefficient of the polyene did not change upon addition of γCD. Such points exist in all three polyene−γCD systems:[11] DPB−γCD at 331 nm, DPH−γCD at 362 nm, and DPO−γCD at 381 nm. The maximum possible r values for the three diphenylpolyenes, measured in vitrified solutions and polymer films, are $r_o = 0.38-0.39$.[12−14] All three Ph−(CH═CH−)$_n$−Ph are totally insoluble in pure water. For this reason we have used as solvent a mixture of water/ethylene glycol, 60/40 by volume, in which these molecules were found to form proper solutions with the following solubilities: DPB, 1.3×10^{-6} M; DPH, 8×10^{-8} M; DPO 4×10^{-8} M. Note that we have found nanotube formation to take place between our three polyenes and γCD in pure water, but we will not elaborate on that. All computer fits and simulations were performed using the program "MicroMath Scientist for Windows", version 2.01, of MicroMath Inc.

III. Results and Discussion

Some relevant spectroscopic data concerning the three polyenes of the present study are listed in Table 1. Although these molecules are consecutive homologues of the series Ph−

S1089-5647(97)02267-0 CCC: $15.00
Published on Web 01/27/1998

TABLE 1: Fluorescence Parameters, Lifetime (τ), Quantum Yield (Φ), and Anisotropy Polarization (r) of DPB, DPH, and DPO in Various Solvents

				DPB			DPH			DPO		
solvent	n_D	ϵ	η	τ (ns)	Φ	r	τ (ns)	Φ	r	τ	Φ	r
hexane	1.372	1.88	0.313	0.467	0.350	0.020	15.9	0.630	*b*	6.20	0.044	*b*
dodecane	1.400	2.00	1.508	0.668	0.490	0.030	13.2	0.660	*b*	6.43	0.052	*b*
ethanol	1.359	24.3	1.078	0.060[a]	0.042[a]	0.167	4.8	0.230	*b*	6.56	0.059	*b*
ethylene glycol	1.429	38.66	21	0.187	0.065	0.323	2.58	0.210	0.110	7.07	0.086	0.088
benzene	1.498	2.28	0.603	0.327	0.275	0.040	7.0	0.760	*b*	6.81	0.089	*b*
chloroform	1.444	4.64	0.542	0.156	0.069	0.110	6.2	0.570	*b*	6.73	0.085	*b*
60/40 w/ethylene glycol	1.375	68.40	3.00	0.08	0.011	0.295	0.355	0.031	0.152	5.0	0.038	0.045

[a] Taken from ref 19. [b] r values of DPH and DPO were below 0.01 because of their long fluorescence lifetimes.

SCHEME 1: Dimensions of α,ω-Diphenylpolyenes and γCD

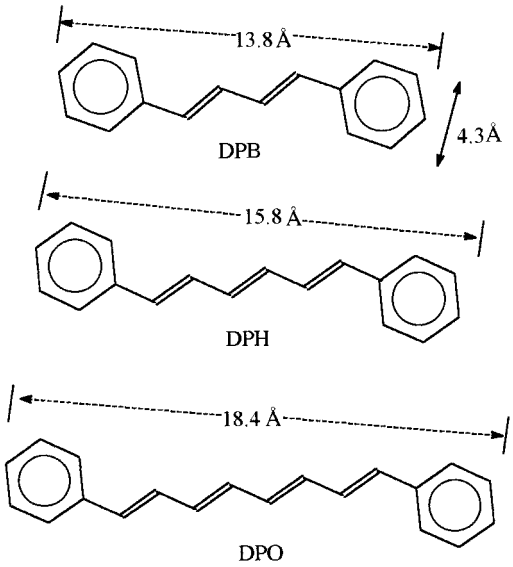

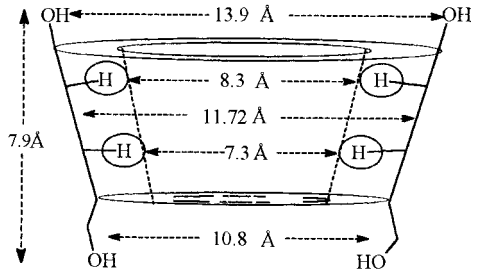

γCD

$(CH{=}CH{-})_n{-}Ph$ with $n = 2,3,4$, they demonstrate, nevertheless, some important differences in their fluorescence parameters, viz., quantum yields (Φ), anisotropies (r), and lifetimes (τ), as shown in Table 1. Thus, although τ and Φ of DPB and DPH depend on the solvent, in DPO they are nearly independent of it. Also, the very low lifetimes of DPB in all solvents make the fluorescence anisotropy of this molecule approximately constant in all media.

Nanotube Formation. The general assumption we have made concerning nanotube formation is that it proceeds as a self-association reaction of the initially formed (DPP)−(γCD) unit. The steps therefore that lead to the formation of a nanotube are described by the following equations (1):

$$\mathrm{DPP} + \gamma\mathrm{CD} \overset{K_{11}}{\rightleftharpoons} (\mathrm{DPP})-(\gamma\mathrm{CD})$$

$$(\mathrm{DPP})-(\gamma\mathrm{CD}) + (\mathrm{DPP})-(\gamma\mathrm{CD}) \overset{K_{22}}{\rightleftharpoons} (\mathrm{DPP})_2-(\gamma\mathrm{CD})_2$$

$$(\mathrm{DPP})_2-(\gamma\mathrm{CD})_2 + (\mathrm{DPP})-(\gamma\mathrm{CD}) \overset{K_{33}}{\rightleftharpoons} (\mathrm{DPP})_3-(\gamma\mathrm{CD})_3$$

$$(\mathrm{DPP})_{i-1}-(\gamma\mathrm{CD})_{i-1} + (\mathrm{DPP})-(\gamma\mathrm{CD}) \overset{K_{ii}}{\rightleftharpoons} (\mathrm{DPP})_i-(\gamma\mathrm{CD})_i \quad (1)$$

On the basis of previous theoretical[15] and experimental[16] studies of chain-association equilibria, we have further assumed that the equilibrium constant K_{ii} for all reactions with $i > 1$ is equal to K; i.e., it is independent of i. Therefore, $K_{22} = K_{33} = \ldots K_{ii} = K$.

It is also conceivable that in addition to eq 1 more reactions of the types described by the equations in (2)

$$(\mathrm{DPP})-(\gamma\mathrm{CD}) + \gamma\mathrm{CD} \overset{K_{12}}{\rightleftharpoons} (\mathrm{DPP})-(\gamma\mathrm{CD})_2$$

$$(\mathrm{DPP})_2-(\gamma\mathrm{CD})_2 + \gamma\mathrm{CD} \overset{K_{23}}{\rightleftharpoons} (\mathrm{DPP})_2-(\gamma\mathrm{CD})_3 \quad (2)$$

and eq 3

$$(\mathrm{DPP})-(\gamma\mathrm{CD}) + \mathrm{DPP} \overset{K_{21}}{\rightleftharpoons} (\mathrm{DPP})_2-(\gamma\mathrm{CD}) \quad (3)$$

can also take place. Therefore, we have included them too in our computer simulations. The concentration of DPP in these simulations was taken to be equal to 5×10^{-8} M in accordance with our water solubility data for the three diphenylpolyenes used here. We should also mention that in our simulations the number of consequent associations in the equations of (1) has been restricted to $i = 10$ because beyond that number our computer program breaks down. Therefore, the longest complex in these simulations will be the $(\mathrm{DPP})_{10}-(\gamma\mathrm{CD})_{10}$. We have set as our criterion for nanotube formation that the magnitudes of the molar fractions f_{ii}, of the longest complexes $(\mathrm{DPP})_i-(\gamma\mathrm{CD})_i$ are large compared with the magnitudes of f_{ii} and f_{ij} of the short complexes $(\mathrm{DPP})_i-(\gamma\mathrm{CD})_i$ and $(\mathrm{DPP})_i-(\gamma\mathrm{CD})_j$. Furthermore, to avoid congestion of our figures we have included in Figures 1 and 2 only the [γCD] dependence of the molar fractions, f_{11}, f_{22}, $f_{10,10}$ obtained from simulations according to the equations of (1) (Figure 1a), f_{12}, f_{23}, $f_{10,10}$ obtained from simulations according to the combined equations of (1) and (2) (Figure 1b), and f_{21} and $f_{10,10}$ from simulations according to the combined equations of (1) and (3) (Figure 2). Note finally that in our notation the first subscript i, in f_{ij}, K_{ij}, etc, corresponds to DPP while the second subscript j to γ-CD. In all computer simulations that follow, the value of the equilibrium constant K_{11} was always set equal to 100 M^{-1}, adopted as an ap-

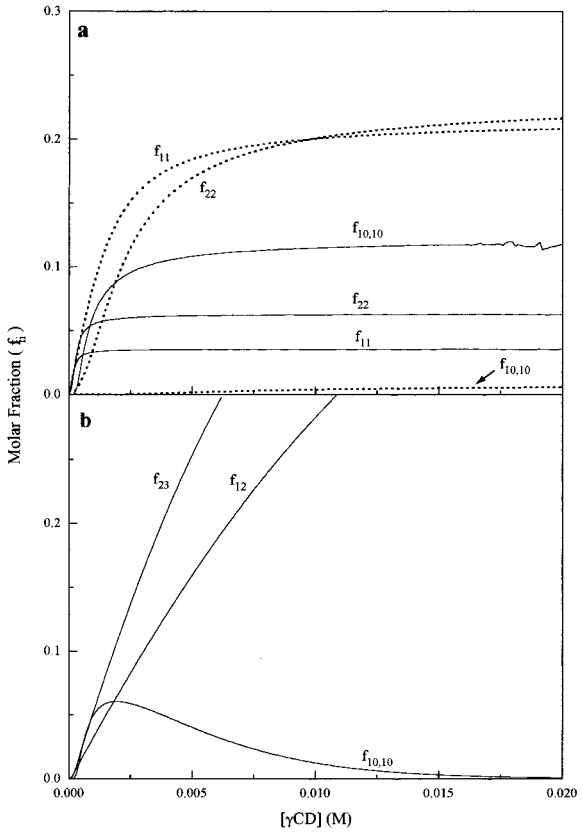

Figure 1. Computer simulations of the molar fraction (f_{ij}) vs cyclodextrin concentration ([γCD]). (a) According to (1) for solid lines, $K_{11} = 100\ M^{-1}$, $K = 5 \times 10^8\ M^{-1}$; for dotted lines, $K_{11} = 100\ M^{-1}$, $K = 5 \times 10^7\ M^{-1}$. (b) According to (1) and (2) with $K_{11} = 100\ M^{-1}$, $K = 5 \times 10^8\ M^{-1}$, $K_{12} = K_{23} = 1000\ M^{-1}$. All simulations were performed for i up to 10 because beyond that point the program broke down.

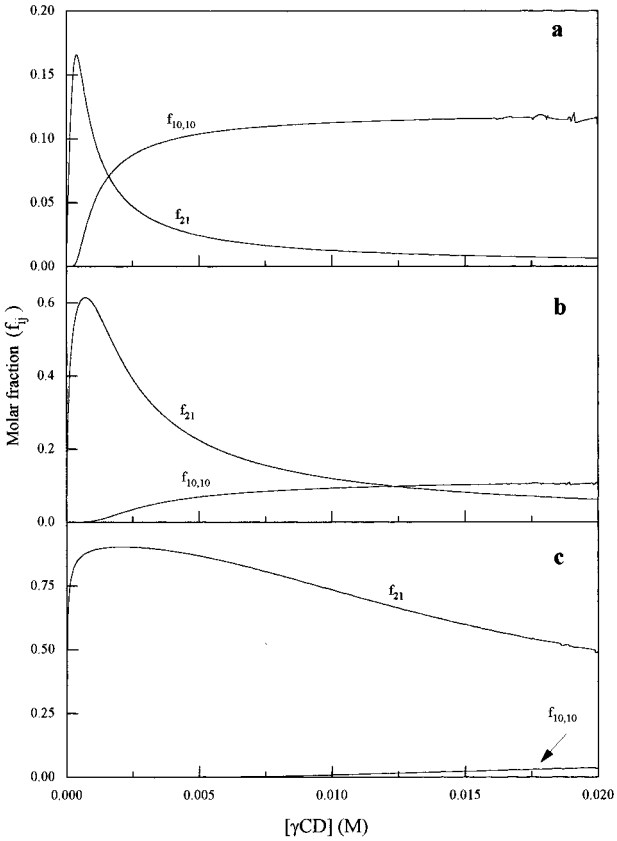

Figure 2. Computer simulations of the molar fraction (f_{ij}) vs cyclodextrin concentration ([γCD]) according to (1) and (3): (a) $K_{11} = 100\ M^{-1}$, $K_{21} = 10^8\ M^{-1}$, $K = 5 \times 10^8\ M^{-1}$; (b) $K_{11} = 100\ M^{-1}$, $K_{21} = 10^9\ M^{-1}$, $K = 5 \times 10^8\ M^{-1}$; (c) $K_{11} = 100\ M^{-1}$, $K_{21} = 10^{10}\ M^{-1}$, $K = 5 \times 10^8\ M^{-1}$. All simulations were performed for i up to 10 because beyond that point the program broke down.

proximately mean value between published data[2] and our unpublished results on the complexation of DPH with and α- and β-cyclodextrins in the same medium, viz., 60/40 water/ethylene glycol.

In Figure 1a the solid lines correspond to the f_{11}, f_{22}, and $f_{10,10}$ obtained according to (1) and for binding constants $K_{11} = 100\ M^{-1}$ and $K = 5 \times 10^8\ M^{-1}$. These plots show that under these conditions nanotubes form, since above a small γCD concentration, ca. 10^{-3} M, $f_{10,10}$ stays larger than f_{11} and f_{22}. The dotted lines in Figure 1a, on the other hand, correspond to the same model of (1) with $K_{11} = 100\ M^{-1}$ but with $K = 5 \times 10^7\ M^{-1}$. These plots show that nanotubes do not form when K assumes some value lower than approximately $10^8\ M^{-1}$, since in this case the magnitude of $f_{10,10}$ is much smaller than those of f_{11} and f_{22}. The plots of Figure 1b correspond to the indicated molar fractions obtained from the combination of (1) and (2) with equilibrium constants $K_{11} = 100\ M^{-1}$, $K_{12} = K_{23} = 1000\ M^{-1}$, and $K = 5 \times 10^8\ M^{-1}$. It is quite clear from these plots that when the side reactions of (2) are included in the simulations, the molar fraction of the long structure, $f_{10,10}$, which accounts for the nanotubes, undergoes a dramatic decrease, while the molar fractions f_{12} and f_{23}, of the $(DPP)_1-(\gamma CD)_2$ and $(DPP)_2-(\gamma CD)_3$ complexes, which terminate nanotube formation, rise sharply. Therefore, nanotubes do not form.

We have also considered the combination of (1) with (3) as shown in the plots of Figure 2, but we found that the effect of this type of interaction is rather unimportant in these systems, as indicated by the low molar fraction f_{21} compared with $f_{10,10}$, for K_{21} values even as high as $10^8\ M^{-1}$. This is understood in terms of the aforementioned very low solubility of DPP in the solvent employed here, ca. 8×10^{-8} M, which requires unreasonably large values of the equilibrium constant K_{21} in order for this reaction to assume a detectable role in the overall nanotube formation. Note that the effect of (3) is demonstrated in the case of the fluorescence quantum yield of the DPB−γCD system (see Figure 4). We conclude therefore that nanotube formation is adequately described by the self-association process of (1) whereas when (2) occurs, nanotubes do not form. Finally, processes of the type in (3) do not have any effect on nanotube formation unless they are assigned an unreasonably large equilibrium constant, viz., $K_{21} > 10^9\ M^{-1}$. All the findings of these simulations are confirmed by the experimental data discussed in the rest of this article. It should also be mentioned here that similar equations describing chain association equilibria in other systems have been reported before.[16]

Figure 3 shows the variation of the fluorescence quantum yield Φ and anisotropy r as the concentration of added γCD increases while keeping constant the concentration of the diphenylpolyenes, viz., [DPB] = 1.3×10^{-6} M, [DPH] = 7×10^{-8} M, [DPO] = 4×10^{-8} M. It becomes evident from these plots that each one of the homologues behaves differently from the others. Thus, in the case of DPB−γCD the quantum yield starts from a very low value, $\Phi = 0.011$, and then rises, slowly at the beginning and then more quickly, until it reaches the value of ca. 0.35 at about 5×10^{-2}M of added γCD. In DPH, Φ starts again from a low value of about 0.031 but then rises quickly to ca. $\Phi = 0.56$ at [γCD] = 1.2×10^{-2} M where it levels off. Finally, in a totally different fashion from the other two polyenes, DPO exhibits low fluorescence quantum yield,

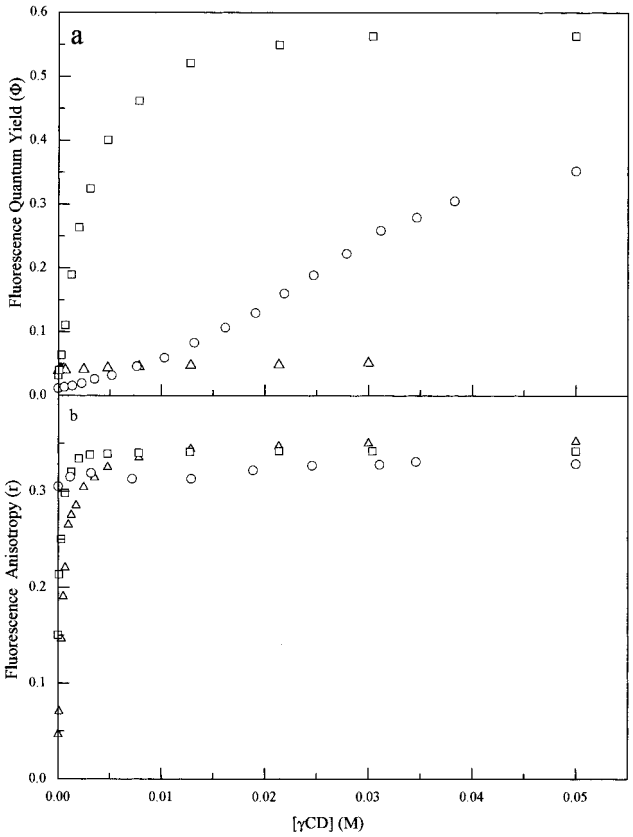

Figure 3. (a) Fluorescence quantum yield (Φ) vs [γCD]; (b) fluorescence anisotropy (r) vs [γCD]. Solvent is 60/40 water/ethylene glycol v/v with (○) DPB, (□) DPH, and (△) DPO.

ca. 0.045, in the entire range of added γCD, $(0-5) \times 10^{-2}$ M. The *r* values also demonstrate different behavior. Thus, while in DPH and DPO the rise of *r* with increasing [γCD] is initially extremely sharp and soon levels off, in the case of DPB all *r* values are equal to ca. 0.31−0.33 for the entire range of [γCD]. Owing to these large differences in behavior among the three different polyene−γCD complexes, it is best to discuss them separately.

DPB−γCD. For DPB in 60/40 water/glycol solvent and a concentration of added γCD equal to 2×10^{-2} M, we have measured two different lifetimes, one equal to 0.2 ns and the other equal to 1.2 ns, the former corresponding to 75% of the DPB molecules and the latter to 25%. From these numbers and the Perrin equation, (4), we have calculated the rotational correlation times τ_c corresponding to the two species, using $r = 0.325$ (see Table 2) and $r_o = 0.39$.[12]

$$r = r_o/(1 + \tau/\tau_c) \tag{4}$$

Introducing then these τ_c values in the Einstein equation, (5), where η is

$$\tau_c = \eta jV/(RT) \tag{5}$$

the viscosity of the medium, *R* the gas constant, *T* the absolute temperature, *V* the molecular volume of the γCD, known from X-ray crystallography,[17] we have determined *j*, the number of the γCD units comprising each nanotube. In this way we have estimated the size of the DPB−γCD complex to be equal to an average of 3.5 γCD units per complex (see Table 2), a structure that by no means can be considered a nanotube. On the other hand, from the dimensions of the γCD cavity and the polyene molecules (see Scheme 1) and also from previous studies,[2] it is concluded that *j* units of γCD arranged in nanotube formation can easily accommodate an equal number of DPB molecules. It is therefore conceivable, in principle, to have in solution all the possible $(DPB)_i-(\gamma CD)_j$ with $i = j = 1-4$. However, we were able to obtain good fits to the Φ vs [γCD] curve (see Figure 4a) by taking into account only the species participating in the reaction of (6):

TABLE 2: Fluorescence Parameters of DPB, DPH, DPO in 2×10^{-2} M γCD (60/40 v/v Water/Ethylene Glycol) and Average Number ⟨*j*⟩ of γCD Units per Nanotube[a]

diphenylpolyenes	Φ	τ (ns)	*f* (mole fraction)	*r*	τ_c (ns)	*jV* (cm³/mol)	⟨*j*⟩
DPB 1.3×10^{-6} M		0.57	0.75		3.4	2780	
	0.35			0.32			3.5
		1.4	0.25	5	8.2	6705	
DPH 8×10^{-8} M		6.1	0.8		55	44900	
	0.56		0.34			37	
		3.5	0.2	2	32	26165	
DPO 4×10^{-8} M		3.27	0.4		43	35160	
	0.05			0.35			50
		6.4	0.6	3	84	68690	

[a] Molecular volume of γCD, $V = 1095$ cm³/mol[10]. $\langle j \rangle = \langle j_1 \rangle f_1 + \langle j_2 \rangle f_2$.

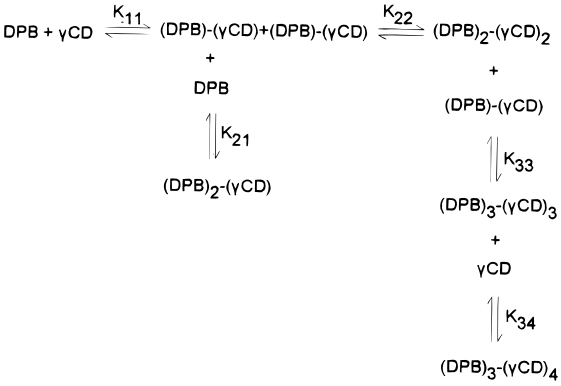

(6)

Attempts to include any other of the possible $(DPB)_i-(\gamma CD)_j$ complexes did not give acceptable fits.

Corresponding to (6) is (7) in which Φ is

$$\Phi = f_f\Phi_f + f_{11}\Phi_{11} + f_{21}\Phi_{21} + f_{22}\Phi_{22} + f_{33}\Phi_{33} + f_{34}\Phi_{34} \tag{7}$$

$$f_{ij} = i[(DPB)_i - (\gamma CD)_j]/[DPB]_T \tag{7a}$$

the total fluorescence quantum yield at any moment during the titration procedure (addition of γCD). Φ_{ij} and f_{ij} represent the quantum yield and the molar fraction of the various $(DPB)_i-(\gamma CD)_j$ adducts, respectively, and $[DPB]_T = 1.3 \times 10^{-6}$ M is the total concentration of DPB. $\Phi_f = 0.011$ stands for the quantum yield of the free (uncomplexed) DPB before any addition of γCD, as measured in the mixed solvent (see Table 1), and f_f is the molar fraction of the free DPB that remains uncomplexed at any moment during the titration. The connection between the concentration of the various $(DPB)_i-(\gamma CD)_j$ species of (6) and the corresponding binding constants K_{ij}, which are the parameters to be determined, is given by the set of equations in (8):

$$[DPB-\gamma CD] = K_{11}[DPB][\gamma CD]$$

$$[(DPB)_2-\gamma CD] = K_{21}[DPB-\gamma CD][DPB] = K_{21}K_{11}[DPB]^2[\gamma CD]$$

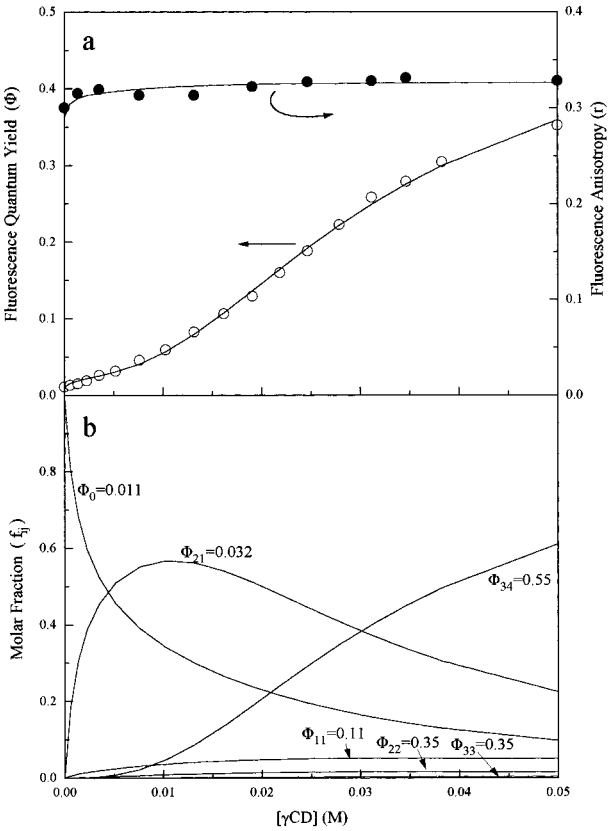

Figure 4. (a) Computer fits of (7) to the Φ vs [γCD] experimental data (□) and of (10) to the *r* vs [γCD] experimental data (○) for DPB. (b) Plot of the molar fractions of the species involved in the fits of (a) vs [γCD]. For fitting parameters see Table 3.

$$[(\mathrm{DPB})_2{-}(\gamma\mathrm{CD})_2] = K_{22}[\mathrm{DPB}{-}\gamma\mathrm{CD}]^2 = K_{22}K_{11}{}^2[\mathrm{DPB}]^2[\gamma\mathrm{CD}]$$

$$[(\mathrm{DPB})_3{-}(\gamma\mathrm{CD})_3] = K_{33}[(\mathrm{DPB})_2{-}(\gamma\mathrm{CD})_2][\mathrm{DPB}{-}\gamma\mathrm{CD}] = K_{33}K_{22}K_{11}{}^3[\mathrm{DPB}]^3[\gamma\mathrm{CD}]^3$$

$$[(\mathrm{DPB})_3{-}(\gamma\mathrm{CD})_4] = K_{34}[(\mathrm{DPB})_3{-}(\gamma\mathrm{CD})_3][\gamma\mathrm{CD}] = K_{34}K_{33}K_{22}K_{11}{}^3[\mathrm{DPB}]^3[\gamma\mathrm{CD}]^4 \quad (8)$$

If the concentrations of the various species, from the above equations of (8), are introduced in (7a) the molar fractions f_{ij} can be expressed in terms of K_{ij}, [DPB], and [γCD]. In addition, the unknown [DPB], i.e., the concentration of the free DPB at any instant during the titration, can also be expressed as a function of K_{ij} and [γCD]. This is accomplished by replacing in (9) which expresses the balance of mass for DPB, the various $[(\mathrm{DPB})_i{-}(\gamma\mathrm{CD})_j]$ terms from (8):

$$[\mathrm{DPB}]_\mathrm{T} = [\mathrm{DPB}] + [\mathrm{DPB}{-}\gamma\mathrm{CD}] + 2[(\mathrm{DPB})_2{-}\gamma\mathrm{CD}] + 2[(\mathrm{DPB})_2{-}(\gamma\mathrm{CD})_2] + 3[(\mathrm{DPB})_3{-}(\gamma\mathrm{CD})_3] + 3[(\mathrm{DPB})_3{-}(\gamma\mathrm{CD})_4] \quad (9)$$

Eventually the (7) assumes its final form in which the experimental parameter Φ is expressed in terms of the desired parameters K_{ij}, Φ_{ij}, and the known quantities [γCD], $[\mathrm{DPB}]_\mathrm{T}$, Φ, Φ_f, f_f, where [γCD] stands for the concentration of the free (uncomplexed) cyclodextrin after each addition of γCD during the titration. Note, however, that since throughout the titration we have used excess γCD relative to polyenes, viz. [γCD]/[DPP] > 10^2, we can assume that at each moment [γCD] is equal to the known analytical cyclodextrin concentration that has been added until then. The final fitting equation is not shown here because it forms an extremely long algebraic expression, while on the other hand, its derivation simply amounts to the above-mentioned straightforward substitutions. Note that similar procedures to express the corresponding fitting equations in terms of the known and of the desired parameters have been also used in the cases of DPH and DPO, and they will not be repeated here. In any case, there are 10 parameters in the modified (but not shown) fitting equation, viz., the binding constants K_{ij} and the quantum yields Φ_{ij} of the five different $(\mathrm{DPB})_i{-}(\gamma\mathrm{CD})_j$ species of (6). Of those 10 parameters only f_f and Φ_f of the free DPB are known (see Table 1). We have further reduced the number of the free-running parameters by 1, assuming that $\Phi_{22} = \Phi_{33}$. The justification for this simplification is that in both species, the $(\mathrm{DPB})_2{-}(\gamma\mathrm{CD})_2$ and the $(\mathrm{DPB})_3{-}(\gamma\mathrm{CD})_3$, the DPB molecules are equally protected from the environment, and therefore, they are expected to have similar quantum yields. The fitting gave the binding constants K_{ij} for each complex $(\mathrm{DPB})_i{-}(\gamma\mathrm{CD})_j$, along with the corresponding fluorescence quantum yields Φ_{ij}, listed in Table 3, and also, through (7a), the dependence of the various molar fractions f_{ij} on [γCD], as shown in Figure 4b.

TABLE 3: Binding Constants and Quantum Yields of the Various Complexes Formed between Diphenylpolyenes and γCD in 60/40 v/v Water/Ethylene Glycol

complex	binding constants K_{ij} (M^{-1})	quantum yields Φ_{ij}	extracted from fits of	goodness of the fit *R*
DPB−γCD	$K_{11} = 11$	$\Phi_{11} = 0.11$	Φ vs [γCD]	
	$K_{21} = 1.7 \times 10^7$	$\Phi_{21} = 0.03$	and *r* vs	0.9993
	$K_{22} = 2.6 \times 10^6$	$\Phi_{22} = 0.35$	[γCD]	
	$K_{33} = 1.0 \times 10^6$	$\Phi_{33} = 0.35$		0.9997
	$K_{34} = 5.8 \times 10^3$	$\Phi_{34} = 0.55$		
DPH−γCD	$K_{11} = 70$[a]	$\Phi_{11} = 0.08$[a]	Φ vs [γCD]	
	$K_{22} = 5 \times 10^8$	$\Phi_{22} = 0.46$[a]		0.999
	$K = 4 \times 10^8$	$\Phi = 0.75$		
DPO−γCD	$K_{11} = 313$	*b*	*r* vs [γCD]	*c*
	$K = 4.2 \times 10^8$			

[a] Values introduced in the program from the literature (see text). [b] Quantum yields do not appear in the fitting equation in this case (see text). [c] Data from simulation.

At this point we may return to the *r* vs [γCD] plot of Figure 3b, and using the information obtained from the fitting of the quantum yields, viz., the complexes $(\mathrm{DPB})_i{-}(\gamma\mathrm{CD})_j$ formed and their molar fractions f_{ij}, we can try to fit the same model of (6) to the *r* vs [γCD] data. The fitting equation in this case is (10) where *r* is the total measured anisotropy at

$$r = I_\mathrm{f}r_\mathrm{f} + I_{11}r_{11} + I_{21}r_{21} + I_{22}r_{22} + I_{33}r_{33} + I_{34}r_{34} \quad (10)$$

any moment during the titration, I_f and I_{ij} refer to the fraction of the total fluorescence intensity due to the free molecule and each one of the $(\mathrm{DPB})_i{-}(\gamma\mathrm{CD})_j$ complexes respectively,[18] $r_\mathrm{f} = 0.295$ is the anisotropy of DPB in the mixed solvent before the addition of any γCD (see Table 1), and r_{ij} is the anisotropy of the $(\mathrm{DPB})_i{-}(\gamma\mathrm{CD})_j$ adduct. Note that r_{ij} is expressible in terms of (4) and (5), since $r_{ij} = \eta r_\mathrm{o} jV/(\eta jV + \tau RT)$ where all factors are known. When the intensity fractions are expressed as $I_{ij} = f_{ij}\Phi_{ij}/\Phi = f_{ij}\phi_{ij}$, where $\phi_{ij} = \Phi_{ij}/\Phi$ represents the ratio of the quantum yield of the particular $(\mathrm{DPB})_i{-}(\gamma\mathrm{CD})_j$ species to the total quantum yield Φ, (10) becomes (11):

$$r = f_\mathrm{f}\phi_\mathrm{f}r_\mathrm{f} + f_{11}\phi_{11}r_{11} + f_{21}\phi_{21}r_{21} + f_{22}\phi_{22}r_{22} + f_{33}\phi_{33}r_{33} + f_{34}\phi_{34}r_{34} \quad (11)$$

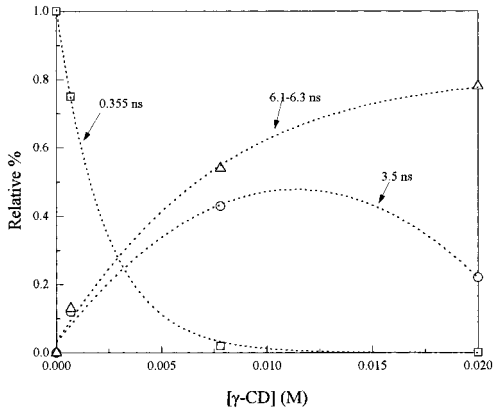

Figure 5. Plots of the relative percentages of the various species found in the DPH and γCD solution in 60/40 water/ethylene glycol vs [γCD]. The species were distinguished by their fluorescence lifetimes, indicated in the plots.

Using the variations of the molar fractions shown in Figure 3b, introducing $\tau = 0.08$ ns for the free DPB (see Table 1), and allowing two more free-running lifetimes, viz., a long one for the $(DPB)_3-(\gamma CD)_4$ complex and a short one for the $(DPB)-(\gamma CD)$ and $(DPB)_2-(\gamma CD)$ complexes, we have obtained for the r vs [γCD] curve the fit shown in Figure 4a, with a very satisfactory criterion for its goodness of fit (the parameters for the goodness of the fits are given in Table 3). The values obtained for the two free-running lifetimes were $\tau = 0.23$ and 0.9 ns, which are very close to the ones obtained from the independent fluorescence-decay measurements mentioned above ($\tau = 0.2$ ns, 75%; $\tau = 1.2$ ns, 25%). Of these two lifetimes, we have assigned the short one to those species that have the DPB more exposed to the solvent, viz. $(DPB)-(\gamma CD)$ and $(DPB)_2-(\gamma CD)$. The longer lifetime we have attributed to the species in which the DPB penetrates the dextrin cavities, and it is therefore protected from the solvent. This is the $(DPB)_3-(\gamma CD)_4$ complex. The above assignments were based on the observation that DPB has a much longer lifetime in hexane than in methanol (Table 1) and that although the solvent water/glycol resembles methanol, the interior of the dextrin cavities is expected to be less polar.

DPH-γCD. The complex formation between DPH and γCD in 60/40 water/glycol leads to a rapid increase of both Φ and r with increasing γCD concentration in the fashion shown in Figure 3. The analysis of the fluorescence decay at various added γCD concentrations gave three different lifetimes. The shortest one, $\tau = 0.36$ ns, corresponds to the free DPH (see Table 1), while the others, $\tau = 3.5$ ns and $\tau = 6.1$ ns, we have assigned to complexes in which the exposure of the DPH to the medium is decreased because of its enclosure in the nanotubes formed by the cyclodextrin cavities. As shown in Figure 5, the fraction of the free DPH, with $\tau = 0.36$ ns, sharply declines with increasing [γCD], the population of the species with $\tau = 3.5$ ns rises and then decreases, while the concentration of the third species with $\tau = 6.1$ ns, which presumably corresponds to the nanotubes, increases continuously. The average length of the DPH$-\gamma$CD structures formed at [γCD] $= 2 \times 10^{-2}$ M, calculated from (4) and (5) and the data of Table 2, was found to correspond to $\langle j \rangle = 37$ cyclodextrin units, which is a genuine nanotube superstructure. Computer fitting of a model, consistent with the above results, to the r vs [γCD] data for DPH shown in Figure 3b is not feasible because of the very large size of these nanotubes and the fact that as the length of the tube increases, with increasing [γCD], its rotational correlation time τ_c increases too.

In the case of Φ vs [γCD] the overall fitting equation is

$$\Phi = f_f \Phi_f + \sum_{i=1}^{37} f_{ii} \phi_{ii} \tag{12}$$

where f_{ii} is given by (7a). The derivation from (12) of the final fitting equation, which is expressed in terms of the known and the unknown parameters, is the same as the derivation for the case of the DPB$-\gamma$CD complex, which was described in terms of (7−9), and therefore, it need not be repeated again. The situation with the fittings here is equally complicated as in the r vs [γCD] case, since there are approximately 37 steps in the nanotube formation, with a different binding constant K_{ii} and a different fluorescence quantum yield Φ_{ii} corresponding to each step. It is possible, however, by making some reasonable simplifications to obtain estimates for the magnitudes of the binding constants involved in this DPH$-\gamma$CD nanotube formation. Thus, we first take into account the fact that nanotube formation proceeds in the self-association fashion of (1) and that for $i \geq 2$ all the binding constants K_{ii} are equal to K. We have also assumed that for $i \geq 2$ all the fluorescence quantum yields are also equal, i.e., $\Phi_{ii} = \Phi$. For the reaction of the first step we have taken the equilibrium constant K_{11} equal to that known from the similar complex (DPH)$-(\alpha$CD), where $K_{11} = 70$ M^{-1},[11] whereas the value of Φ_{11} for the quantum yield of the 1:1 complex, was set equal to the known quantum yield of the DPH$-\beta$CD[11] complex, viz., $\Phi_{11} = 0.08$. The fits obtained in this way, however, were not very good. For this reason we introduced two more parameters, the binding constant K_{22}, as free-running, and the corresponding quantum yield Φ_{22} to which we assigned the value 0.45 known from the similarly structured complex $(DPH)_1-(\alpha CD)_2$.[11] The new fitting was acceptable and the parameters obtained very reasonable, viz., $K_{22} = 5 \times 10^8$, $K = 4 \times 10^8$ M^{-1} and $\Phi = 0.75$. The fact that K_{22} turned out to be of the same order of magnitude as K confirms that the assumption made in discussing (1) namely, that all binding constants K_{ii} for $i \geq 2$ are set approximately equal to K, is correct. On the other hand the value 0.75 found for the quantum yield Φ is the same as the quantum yield of DPH in benzene. This is very reasonable, since, from absorption and fluorescence spectra, we have found[11] that the environment in the interior of the nanotubes resembles very much that of pure benzene. Finally, it is worth mentioning that our attempts to make the above fittings $\langle i \rangle = \langle j \rangle = 37$ caused a breakdown of the program. For this reason we made several fits, one example of which is shown in Figure 6, increasing the number of steps from three up to the point where the program starts breaking down. We found that the program can work up to 18 steps and that for steps more than 6, the parameters extracted turn out to have the same values. All the parameters obtained from these fittings are listed in Table 3.

DPO-γCD. Obviously, there is little information provided by the flat Φ vs [γCD] plot for the case of DPO$-\gamma$CD in Figure 3a. In fact, there is no evidence even that complexation between this polyene and γCD takes place. It is only because of the r vs [γCD] plot of Figure 3b that we know of the complex formation between DPO and γCD. Here, we have again adopted the self-association scheme of (1) and following the same derivation as for (11), we have obtained (13) as the fitting equation for the fluorescence anisotropy r vs [γCD] of DPO$-\gamma$CD nanotubes.

$$r = f_f \phi_f r_f + \sum_{i=1}^{50} f_{ii} \phi_{ii} r_{ii} \tag{13}$$

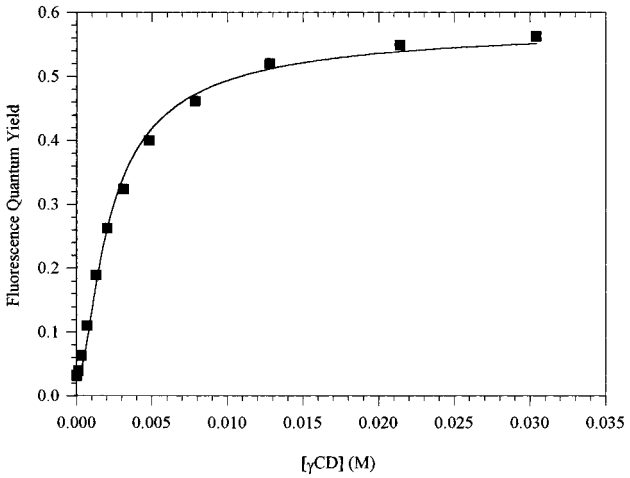

Figure 6. Computer fit of (12) to the fluorescence quantum yield data of DPH vs [γCD]. Solvent is 60/40 water/ethylene glycol. For fitting parameters see Table 3.

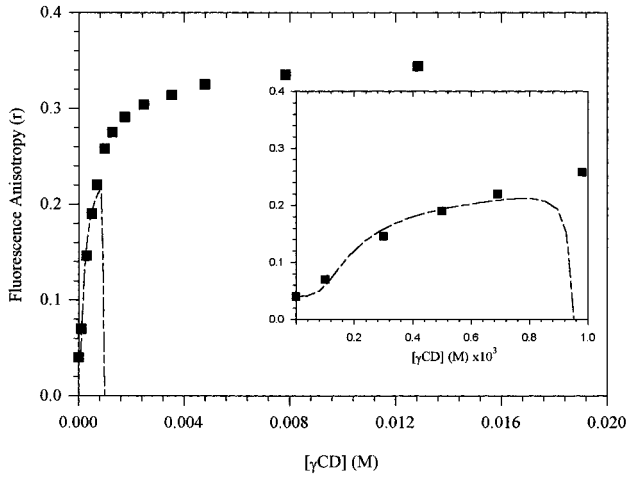

Figure 7. Computer fit of (14) to the fluorescence anisotropy vs [γCD] data. The fitting was performed with $i = 30$, but the calculations broke down as shown. The inset shows the details of the fit at very low [γCD].

All the parameters in (13) have the same meaning as those in (11) viz., r_{ii} is the fluorescence anisotropy of the complex $(DPO)_i-(\gamma CD)_i$, $\phi_{ii} = \Phi_{ii}/\Phi$ is the ratio of the fluorescence quantum yield Φ_{ii} of the species $(DPO)_i-(\gamma CD)_i$ to the total quantum yield Φ, and f_f and ϕ_f refer to the free DPO molecule. Moreover, since the quantum yield of DPO is independent of complex formation with γCD (compare the flat Φ vs [γCD] curve for DPO in Figure 3a), ϕ_f and ϕ_{ii} can be set equal to unity. Therefore, (13) takes the form of (14), which is a simplified expression of the fitting equation. This was further manipulated, in the same way as for (7)−(11), to produce the final fitting equation (not shown) in terms of known parameters and the unknown binding constants.

$$r = f_f r_f + \sum_{i=1}^{30} f_{ii} r_{ii} \qquad (14)$$

From the fluorescence lifetimes of $(DPO)_i-(\gamma CD)_i$ during the titration, we have calculated, by means of (4) and (5), the contribution to the overall value of r of the fluorescence anisotropy r_{ii} of each one of the $(DPO)_i-(\gamma CD)_i$ adducts, for $i = 1-30$. The values of i did not extend to 50, the mean number of the γCD unit per nanotube, because we found that for i above ca. 30 the program was consistently breaking down. Figure 7 shows computer fittings of the data r vs [γCD] for the DPO−γCD nanotubes. The program soon breaks down, as also indicated in Figure 7, but still the fitting is very good in the small γCD concentration range, before the failure of the program, where even the initial slight upward curvature of the experimental points is reproduced (see insert in Figure 7). The parameters obtained in this case from the computer fits do not involve the fluorescence quantum yields, since the Φs were eliminated from the fitting equation of (14).

IV. Conclusions

The main conclusions of the present study may be summarized as follows. (1). The effect of the length of the diphenylpolyene turns out to be very important for nanotube formation. Thus, DPB, the shortest homologue, does not induce formation of long tubes, DPH facilitates the formation of tubes consisting of up to ca. 37 γCD units, whereas DPO produces the largest structures with ca. 50 cyclodextrin units. (2) Nanotube formation between γCD and α,ω-diphenylpolyenes proceeds as a self-associative chain reaction, each step of which consists of the attachment of one DPP-γCD unit to the growing nanotube. (3) The binding constant K_{11} of the very first step, viz., the formation of the DPP−γCD unit, increases from ca. 10 to 300 M^{-1} as the length of the polyene increases from $n = 2$ to $n = 4$. (4) The binding constants K for the rest of the interactions turn out to be independent of the length of the polyene (at least for $n = 3$ and $n = 4$), and to be consistently above ca. 1×10^8 M^{-1}, while for lower K values nanotubes do not form. (5) Attachment of one dextrin molecule to the $(DPP)_i-(\gamma CD)_i$ growing complex has detrimental effects on nanotube formation, whereas attachment of one DPP to the chain of the growing nanotube does not seem to have any effect.

References and Notes

(1) Wenz, G. *Angew. Chem., Int. Ed. Engl.* **1994**, *33*, 803.
(2) Pistolis, G.; Malliaris, A. *J. Phys. Chem.* **1996**, *100*, 15562.
(3) Li, G.; McGown, L. B. *Science* **1994**, *264*, 249.
(4) Gibson, H. W.; Bheda, M. C.; Engen, P. T. *Prog. Polym. Sci.* **1994**, *19*, 843.
(5) Harada, A.; Li, J.; Kamachi, M. *Nature* **1992**, *356*, 325.
(6) Harada, A.; Li, J.; Kamachi, M. *Nature* **1993**, *364*, 516.
(7) Born, M.; Ritter, H. *Angew. Chem., Int. Ed. Engl.* **1995**, *34*, 309.
(8) Harada, A. *Supramol. Sci.* **1996**, *3*, 19.
(9) Yamaguchi, I.; Osakada, K.; Yamamoto, T. *J. Am. Chem. Soc.* **1996**, *118*, 1811.
(10) Pistolis, G.; Malliaris, A. *Langmuir* **1997**, *13*, 1457.
(11) Pistolis, G.; Malliaris, A. To be published.
(12) Anderton, R. M.; Kauffman, J. F. *J. Phys. Chem.* **1994**, *98*, 12117.
(13) Shinitzky, M.; Barenhof, Y. *J. Biol. Chem.* **1974**, *249*, 2652.
(14) Kawski, A.; Kubicki, A.; Kuklinski, B.; Piszczek, G. *Z. Naturforsch.* **1993**, *48a*, 947.
(15) Sarolea-Mathot, L. *Trans. Faraday Soc.***1953**, *49*, 8.
(16) LaPlanche, L. A.; Thompson, H. B.; Rogers, M. T. *J. Phys. Chem.* **1965**, *69*, 1482.
(17) Harata, K. *Bull. Chem. Soc. Jpn.* **1987**, *60*, 2763.
(18) Lakowicz, J. R. *Principles of Fluorescence Spectroscopy*; Plenum Press: New York, 1983; p 145.
(19) Velsko, S. P.; Fleming, G. R. *J. Chem. Phys.* **1982**, *76*, 3553.